

Spatial mode properties of plasmon assisted transmission

Xi-Feng Ren, Guo-Ping Guo¹, Yun-Feng Huang, Zhi-Wei Wang, Guang-Can Guo

Key Laboratory of Quantum Information and Department of Physics, University of Science and Technology of China, Hefei 230026, People's Republic of China

Orbital angular momentum of photons is explored to study the spatial mode properties of plasmon assisted transmission process. We found that photons carrying different orbital angular momentums have different transmission efficiencies, while the coherence between these spatial modes can be preserved.

© 2018 Optical Society of America

OCIS codes: 230.3990, 240.6680, 030.1640.

It has long been observed that there is an unusually high optical transmission efficiency in metal films perforated with a periodic array of subwavelength apertures.¹ Generally, it is believed that metal surface plays a crucial role and the phenomenon is mediated by surface plasmons (SPs) and there is a process of transform photon to surface plasmon and back to photon.²⁻⁴ In 2002, E. Altewischer *et al.*⁵ first addressed the question of whether the entanglement survives in this extraordinary enhancement light transmission. They showed that quantum entanglement of photon pairs can be preserved when they respectively travel through a hole array. Therefore, the macroscopic surface plasmon polarizations, a collective excitation wave involving typically 10^{10} free electrons propagating at the surface of conducting matter, have a true quantum nature.

So far, polarization properties of nanohole arrays have been studied in many works.⁶⁻⁸ Then, how about the spatial mode properties of nanohole arrays in the photon to plasmon and back to photon process? The metal plates used in previous experiments always have special structure-usually like lattice. Modes of surface plasmons are correlated with these typical structures. If the light incidented on the metal plate has a transverse spatial distribution itself, what will happen? What are the spatial modes of the transmitted photons? Understanding these questions will help us to have an in-depth understanding on the plasmon-assisted transmission process. In our experiment, photons with different orbital angular momentums (OAM) are incidented on the metal plate and OAM of transmitted

¹gpguo@ustc.edu.cn

photons of zero-order are investigated. We find that for photons carrying integral OAM, the spatial modes are not changed, while different OAM corresponding to different transmission efficiencies. The coherence between different spatial modes can also be preserved.

Fig. 1 shows the metal plate transmittance as a function of wavelength. The dashed vertical line indicates the wavelength of 670 nm used in our experiment. The transmission efficiency of the metal plate at 670 nm is about 2.5%, which is much larger than the value of 0.55% obtained from classical theory.⁹ The metal plate is produced as follows: after subsequently evaporating a 3-nm titanium bonding layer and a 135-nm gold layer onto a 0.5-mm -thick silica glass substrate, a Focused Ion Beam Etching system (FIB, DB235 of FEB Co.) is used to produce cylindrical holes (200 nm diameter) arranged as a square lattice (600 nm period). The total area of the hole array is $30\mu\text{m} \times 30\mu\text{m}$, which is actually made up of four hole arrays of $15\mu\text{m} \times 15\mu\text{m}$ area for the technical reason.

It has been shown that paraxial Laguerre-Gaussian(LG) laser beams carry a well-defined OAM,¹⁰ and LG modes form a complete Hilbert space. If the mode function is a pure LG mode with winding number l , then every photon of this beam carries an OAM of $l\hbar$. This corresponds to an eigenstate of the OAM operator with eigenvalue $l\hbar$.¹⁰ If the mode function is not a pure LG mode, each photon of this light is in a superposition state, with the weights dictated by the contributions of the comprised different l th angular harmonics.

Usually, we use computer generated holograms (CGHs)^{11–13} to change the winding number of LG mode light. It is a kind of transmission holograms. Corresponding to the diffraction order m , the hologram can change the winding number of the input beam by $\Delta l_m = ml$. The diffraction efficiency depends on the phase modulation δ . In our experiment, the efficiencies of CGHs are all about 30%. Fig. 2. shows part of a typical CGH($l = 1$) with a fork in the center. Generally, it is also important to be able to both produce and analyze superposition states in a chosen basis. A convenient method for creating superposition modes is to use a displaced hologram,¹² which is particularly suitable for producing superpositions of an LG_{0l} mode with the Gaussian mode. The Gaussian mode ($l = 0$) can be identified using single-mode fibers in connection with avalanche detectors. All other modes have a larger spatial extension, and therefore cannot be coupled into the single-mode fiber efficiently. High order LG modes ($l \neq 0$) are identified using mode detectors consisting of CGH and single-mode optical fiber(Shown in Fig. 2.). This mode detector can also be used to identify the superposition mode by displace the CGH.^{12,14}

The experimental setup is shown in Fig. 2. The light is in vertical polarization with 670 nm wavelength. A CGH ($\Delta l = 1$) is used to change OAM of the light from output of a single-mode fiber. The metal plate is placed between the twin lenses(focus 35 mm), so the light incidented on the metal plate has a diameter about $25\mu\text{m}$. Another CGH ($\Delta l = -1$) and single-mode fiber are combined to analyze the OAM of the transmitted photons. Silicon

avalanche photodiode (APD) photon counter is used to record counts (We use neutral density filter to reduce the intensity of transmitted zero-order light). First of all, we remove the metal plate from the twin-lenses. When the fork of first CGH is placed far away from the beam center, OAM of the light is not changed and the photons are still in OAM state $|0\rangle$. In this case, we move the second CGH from one side to another side horizontally and record the counts. Fig. 3(a) shows the experiment result, which fits nicely with the theoretical numerical calculation. Then the first CGH is placed with the fork in beam center, which changes the OAM state of photons to $|1\rangle$. We also move the second CGH from one side to another side horizontally and record the counts. The experiment result is shown in Fig. 3(b), which also fits nicely with the numerical calculation. These results show that the shifted holograms work as described above.

Now we put the metal plate with hole array between the twin lenses. Firstly, We move the second CGH horizontally and record the counts with photons of Gaussian mode incidented on the metal plate. As shown in Fig. 4(a), the counts have a similar curve which indicates the spatial mode of the light is not changed, OAM state of the transmitted photon is also $|0\rangle$. For the cases that input photons in OAM states $|1\rangle$ or $|-1\rangle$ (not shown in Fig. 4.), the spatial modes are also preserved. So the spatial modes are not changed for photons carrying integral OAM. It is also found that for different OAM modes light, the transmission efficiencies are different. For light in $|0\rangle$ OAM state, the transmission efficiency is $2.27 \pm 0.27\%$; while for light in $|1\rangle$ ($|-1\rangle$) OAM state, the transmission efficiency is $1.56 \pm 0.02\%$ ($1.42 \pm 0.10\%$).

To investigate the decoherence between different modes in the photon to plasmon and back to photon process, we need to input superposition mode light on the metal plate. In the experiment, it is done by displacing the fork of first CGH from the beam center. The incident OAM state on the metal plate is $(a|0\rangle + b|1\rangle)/\sqrt{a^2 + b^2}$, where a and b are real numbers. In the case of no metal plate, if we move the second hologram from one side to another side horizontally, there must be a special place that we have no count. Because in this special place the second hologram change the state of input light from $(a|0\rangle + b|1\rangle)/\sqrt{a^2 + b^2}$ to $(m|1\rangle + n|-1\rangle)/\sqrt{m^2 + n^2}$, which can not be transmitted by single-mode fiber. The counts are shown in Fig. 5(a) with visibility 96.0%. Then we place the metal plate between the twin-lenses. If there is decoherence between different OAM states (here $|0\rangle$ and $|1\rangle$), there should be a random phase $\varphi(t)$ between $|0\rangle$ and $|1\rangle$ of output photons from metal plate (This random phase actually corresponds to a dephasing process). The state will change to $(a'|0\rangle + e^{i\varphi(t)}b'|1\rangle)/\sqrt{a'^2 + b'^2}$, where a' and b' are real numbers. Then however we move the second CGH, we can always have counts for counts in experiment corresponding to sum of coming photons in a period of time. On the contrary, if there is no decoherence (or dephasing), we can also find a position of the second CGH where there is no count. The experimental result is shown in Fig. 5(b). We still find the no-count place, and the visibility

is 94.4%. There is a small distance between this no-count place and the no-count place with no metal plate (Shown in Fig. 5), which is coming from the different transmission efficiencies of different modes light. The coherence between state $|0\rangle$ and state $|-1\rangle$ is also investigated by changing the CGHs. The visibilities without and with the metal plate are 81.9% and 82.0% respectively. So we can say, the coherence between different modes is preserved and there is no dephasing between different OAM states in this plasmon assisted transmission.

In conclusion, we have investigated the spatial mode properties of our typical nanohole arrays in the photon to plasmon and back to photon process. We found that for photons carrying integral OAM, the spatial mode is not changed, while the transmission efficiencies for different modes light are different. The efficiencies are concerned with the spatial distribution of the input light. A more interesting phenomenon is that the coherence between different modes is preserved. These results may give us more hints to the understanding of plasmon-assisted transmission of photons.

Acknowledgments

This work was funded by the National Fundamental Research Program (2001CB309300), National Nature Science Foundation of China (10304017), the Innovation Funds from Chinese Academy of Sciences and the Program of the Education Department of Anhui Province (Grant No.2006kj074A).

References

1. T.W. Ebbesen, H. J. Lezec, H. F. Ghaemi, T. Thio, and P. A. Wolff, *Nature* 391, 667 (1998).
2. H. Raether, *Surface Plasmons on Smooth and Rough Surfaces and on Gratings*, *Springer Tracts in Modern Physics*, Springer, Berlin, 1988 Vol. 111.
3. D. E. Grupp, H. J. Lezec, T. W. Ebbesen, K. M. Pellerin, and Tineke Thio, *Appl. Phys. Lett.* 77 1569 (2000).
4. M. Moreno, F. J. Garca-Vidal, H. J. Lezec, K. M. Pellerin, T. Thio, J. B. Pendry, and T. W. Ebbesen, *Phys. Rev. Lett.* 86, 1114 (2001).
5. E. Altewischer, M. P. van Exter and J. P. Woerdman, *Nature* 418 304 (2002).
6. J. Elliott, I. I. Smolyaninov, N. I. Zheludev, and A. V. Zayats, *Opt. Lett.* 29, 1414 (2004).
7. R. Gordon, A. G. Brolo, A. McKinnon, A. Rajora, B. Leathem, and K. L. Kavanagh, *Phys. Rev. Lett.* 92, 037401 (2004).
8. E. Altewischer, C. Genet, M. P. van Exter, and J. P. Woerdman, *Opt. Lett.* 30, 90 (2005).
9. H. A. Bethe, *Phys. Rev.* 66, 182 (1944).
10. L. Allen, W. Beijersbergen, R. J. C. Spreeuw and J. P. Woerdman, *Phys. Rev. A* 45 8185 (1992).

11. J. Arlt, K. Dholakia, L. Allen and M. J. Padgett, *J. Mod. Opt.* 45 1231 (1998).
12. A. Vaziri, G. Weihs, A. Zeilinger, *J. Opt. B: Quantum Semiclass. Opt* 4 s47 (2002).
13. X. F. Ren, G. P. Guo, B. Yu, J. Li, and G. C. Guo, *J. Opt. B: Quantum Semiclass. Opt* 6 243 (2004).
14. N. K. Langford, R. B. Dalton, M. D. Harvey, J. L. O'Brien, G. J. Pryde, A. Gilchrist, S. D. Bartlett, and A. G. White, *Phys.Rev.Lett.* **93**, 053601, (2004).

List of Figure Captions

Fig. 1. Hole array transmittance as a function of wavelength. The dashed vertical line indicates the wavelength of 670nm used in the experiment.

Fig. 2. Experimental set-up. A computer generated hologram(CGH) is used to change OAM of the light from output of a single-mode fiber(SMF). The metal plate(MP) is placed between the twin lenses(focus 35mm). The light incident on the metal plate has a diameter small than $30\mu m$. Another CGH and SMF are combined to analyze the OAM of the transmitted photons. Inset, picture of part of a typical CGH($l = 1$).

Fig. 3. Counts(square dots) as a function of the displacement of the second CGH. The metal plate is moved out. (a) The fork of first CGH is displaced far away from the beam center, so the light is in $|0\rangle$ OAM state. (b) The fork of first CGH is placed in the beam center, so the light is in $|1\rangle$ OAM state. The round dots come from theoretical calculation.

Fig. 4. Counts(square dots) as a function of the displacement of the second CGH. The metal plate is placed between the twin-lenses. (a) The fork of first CGH is displaced far away from the beam center, so the light incident on the metal plate is in $|0\rangle$ OAM state. (b) The fork of first CGH is placed in the beam center, so the light incident on the metal plate is in $|1\rangle$ OAM state. The round dots come from theoretical calculation.

Fig. 5. Counts as a function of the displacement of the second CGH. The fork of first CGH is displaced a small amount from the beam center, so the light is in superposition mode.(a) The metal plate is moved out from the twin-lenses. The visibility is 96.0%.(b) The metal plate is placed between the twin-lenses. The visibility is 94.4%.

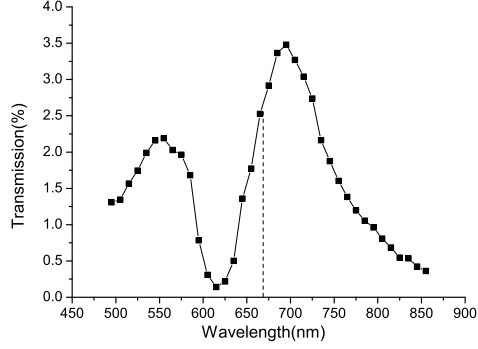


Fig. 1. Hole array transmittance as a function of wavelength. The dashed vertical line indicates the wavelength of 670nm used in the experiment.

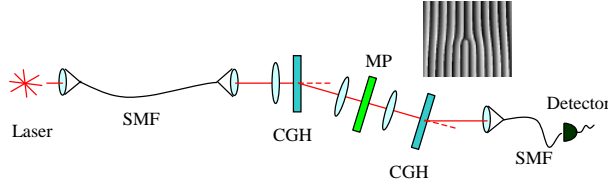


Fig. 2. Experimental set-up. A computer generated hologram(CGH) is used to change OAM of the light from output of a single-mode fiber(SMF). The metal plate(MP) is placed between the twin lenses(focus 35mm). The light incident on the metal plate has a diameter small than $30\mu m$. Another CGH and SMF are combined to analyze the OAM of the transmitted photons. Inset, picture of part of a typical CGH($l = 1$).

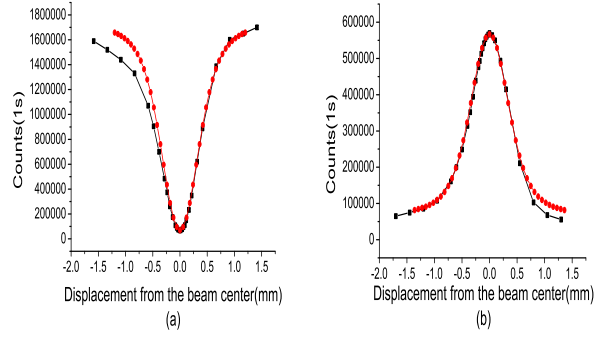


Fig. 3. Counts(square dots) as a function of the displacement of the second CGH. The metal plate is moved out. (a) The fork of first CGH is displaced far away from the beam center, so the light is in $|0\rangle$ OAM state. (b) The fork of first CGH is placed in the beam center, so the light is in $|1\rangle$ OAM state. The round dots come from theoretical calculation.

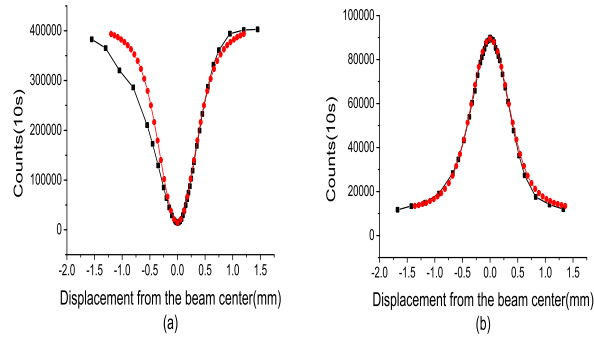


Fig. 4. Counts(square dots) as a function of the displacement of the second CGH. The metal plate is placed between the twin-lenses. (a) The fork of first CGH is displaced far away from the beam center, so the light incident on the metal plate is in $|0\rangle$ OAM state. (b) The fork of first CGH is placed in the beam center, so the light incident on the metal plate is in $|1\rangle$ OAM state. The round dots come from theoretical calculation.

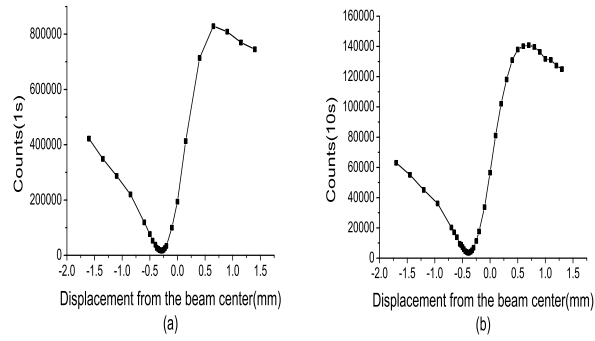


Fig. 5. Counts as a function of the displacement of the second CGH. The fork of first CGH is displaced a small amount from the beam center, so the light is in superposition mode. (a) The metal plate is moved out from the twin-lenses. The visibility is 96.0%. (b) The metal plate is placed between the twin-lenses. The visibility is 94.4%.